available at www.sciencedirect.com

SCIENCE DIRECT®

journal homepage: www.elsevier.com/locate/biochempharm

Pyridine N-oxide derivatives inhibit viral transactivation by interfering with NF-κB binding

Miguel Stevens, Christophe Pannecouque, Erik De Clercq, Jan Balzarini *

Rega Institute for Medical Research, Katholieke Universiteit Leuven, Minderbroedersstraat 10, B-3000 Leuven, Belgium

ARTICLE INFO

Article history:
Received 1 November 2005
Accepted 20 December 2005

Keywords:
Pyridine *N*-oxide derivatives
Human immunodeficiency virus
Cytomegalovirus
Transactivation
NF-κB
Redox regulation

Abbreviations:
BSO, buthionine sulfoximine
CMV, cytomegalovirus
DCFH-DA, 2′,7′-dichlorofluorescein diacetate
DTT, dithiothreitol
EMSA, electrophoretic mobility shift assay
GFP, green fluorescent protein
HIV, human immunodeficiency virus
IκBα, inhibitor of NF-κB
LTR, long terminal repeat
M/M, human primary monocytes/macrophages
NAC, *N*-acetyl-L-cysteine
NF-κB, nuclear factor κB
NNRTI, non-nucleoside reverse transcriptase inhibitor
TNF-α, tumor necrosis factor α
TRX, thioredoxin

ABSTRACT

Pyridine *N*-oxide derivatives represent a new class of anti-HIV compounds for which some members exclusively inhibit HIV-1 RT, whereas other members act, additionally or alternatively, at a post-integrational event in the replicative cycle of HIV. A prototype pyridine *N*-oxide derivative, JPL-32, inhibited tumor necrosis factor alpha (TNF-α)-induced HIV-1 expression in latently HIV-1-infected OM-10.1 and U1 cells, which could be reversed by the addition of *N*-acetyl-L-cysteine (NAC). The reversal of the antiviral activity of JPL-32 by NAC suggested the possible role of a redox-sensitive factor as target of inhibition. Indeed, when nuclear extracts of TNF-α-stimulated OM-10.1 and U1 cells cultured in the presence of JPL-32 were analyzed by an electrophoretic mobility shift assay (EMSA), a dose-dependent inhibition of DNA binding of nuclear NF-κB was observed, which could be reversed by the addition of NAC. JPL-32 did not inhibit the release and subsequent degradation of IκBα, nor did JPL-32 affect the nuclear translocation of NF-κB. EMSA revealed that the inhibition of the NF-κB DNA binding activity by JPL-32 could be reversed by the addition of reducing agents such as dithiothreitol or β-mercaptoethanol. Moreover, JPL-32 was able to directly oxidize the thiol groups on the purified p50 subunit of recombinant NF-κB. The oxidative modification of the thiol groups on NF-κB by JPL-32 could be ascribed to the intracellular pro-oxidant effect of JPL-32. Consequently, JPL-32 was able to increase the intracellular glutathione (GSH) levels and to induce apoptosis in a dose-dependent way.

* *Corresponding author*. Tel.: +32 16 337352; fax: +32 16 337340.
E-mail address: jan.balzarini@rega.kuleuven.be (J. Balzarini).
0006-2952/$ – see front matter
doi:10.1016/j.bcp.2005.12.025

1. Introduction

The NF-κB transcription factor is an ubiquitous redox-sensitive factor that regulates the expression of various genes involved in apoptosis, viral replication, tumor genesis, various autoimmune diseases and inflammation [2,22]. Because of its role in the pathogenesis of various diseases, NF-κB is a target of current interest [28,29]. As part of stress response, NF-κB has been found to be activated in many cell types in response to a broad range of stimuli and conditions, which typically include viral and bacterial products, T- and B-cell mitogens and inflammatory cytokines such as IL-1 and TNF-α [6,17]. NF-κB exists in the cytoplasm of unstimulated cells as a latent form of a transcriptionally active p50/p65 dimer bound to an inhibitory protein, IκBα. Activation of NF-κB involves the phosphorylation of IκBα on two serine residues (S32 and S36), which targets the inhibitor protein for ubiquitination and subsequent degradation by the 26S proteasome [39]. Upon release of IκBα, the nuclear localization signal (NLS) on the p65 subunit becomes unmasked, which allows for a rapid translocation of NF-κB into the nucleus [5]. Once in the nucleus, a cellular reducing catalyst thioredoxin (TRX) plays a major role in stimulation of the DNA binding of NF-κB by reduction of a disulphide bond involving cysteine 62 on the p50 subunit [16,18,24,25]. Although the activation of NF-κB through the release and degradation of IκBα have been shown to occur under oxidative conditions, the binding of NF-κB to the LTR promoter seems to be dependent on reducing conditions, mainly determined by the GSH/GSSG ratio [33,38].

A novel class of pyridine *N*-oxide derivatives were reported to be inhibitory to both HIV-1 and HIV-2 replication, as well as to simian immunodeficiency virus (SIV) and cytomegalovirus (CMV) replication [3,4]. Several members of this class of compounds functionally interact with HIV-1 reverse transcriptase (RT) as typical non-nucleoside RT inhibitors (NNRTIs), whereas other members retain pronounced antiviral potency against HIV-2 and mutant HIV-1 strains, bearing NNRTI-characteristic RT mutations. The latter pyridine *N*-oxide derivatives exert their antiviral activity by a second mechanism of action independent from HIV-1 RT and located at a post-integrational step in the replicative cycle of HIV [35,36]. The prototype pyridine *N*-oxide that acts at a post-integrational event, JPL-32, was recently demonstrated to be endowed with protective activity against HIV-induced $CD4^+$ T cell death in hu-PBMC SCID mice [4]. In the present study, we have outlined the underlying molecular mechanism that explains the inhibitory effect of this compound against viral replication. We show that JPL-32 directly prevents NF-κB DNA binding by oxidative modulation of the p50 subunit of NF-κB.

2. Materials and methods

2.1. Compounds and plasmid constructs

The pyridine *N*-oxide JPL-32 (Fig. 1) was synthesized at, and supplied by, Crompton Corporation, and was dissolved in DMSO to prepare stock solutions at 10 mg/ml (Middlebury, CT and Guelph, Canada). Plasmids used in this study include pHIV-GFPemd that contains the GFP reporter gene driven by the HIV-1 LTR promoter [9], pCMV-GFPemd that contains the EcoRI-SmaI fragment from pCMVβ (BD Biosciences, San Jose, CA) inserted in the EcoRI-StuI sites of the pGFPemd-p vector (Packard).

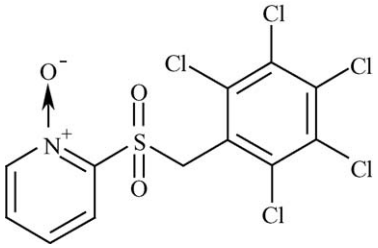

Fig. 1 – Structural formula of JPL-32.

2.2. Cells and viruses

The latently HIV-1-infected promyelocytic OM-10.1 cell line [7] and the latently HIV-1-infected promonocytic U1 cells [14] were maintained in RPMI-1640 medium (Life technologies, Merelbeke, Belgium), supplemented with 10% heat-inactivated fetal calf serum (FCS, Integro, Zaandam, The Netherlands), 2 mM L-glutamine (Life technologies) and 0.1% $NaHCO_3$ (Life technologies), and incubated at 37 °C in a humidified CO_2-controlled atmosphere. HL_{tat} cells (obtained from Dr. B.K. Felber and Dr. G.N. Pavlakis; National Institutes of Health, Bethesda, MD) and $Jurkat_{tat}$ cells [8] are stably expressing HIV-1 Tat protein which is the viral transcriptional activator for mediating HIV-1 transactivation. HL_{tat} cells were maintained in Dulbecco's modified Eagle's medium (DMEM) supplemented with 10% FCS and $Jurkat_{tat}$ cells were maintained in RPMI-1640 medium containing 10% FCS, 2 mM L-glutamine and 0.1% $NaHCO_3$.

2.3. Cytotoxicity and antiviral activity assays

The anti-HIV activity assessment of the pyridine *N*-oxide JPL-32 against chronic HIV-1 infection was based on the inhibition of p24 antigen production in OM-10.1 and U1 cells after stimulation with TNF-α (Roche Diagnostics Belgium). Briefly, OM-10.1 and U1 cells (5×10^5 cells/ml) were incubated in the presence or absence of the compound for 2 h in 48-well plates. After this short incubation period, the cell cultures were stimulated with 1 ng/ml of TNF-α followed by transfer of two times 200 μl into a 96-well plate for cytotoxicity evaluation. After a 2-day incubation at 37 °C, the cell culture supernatants were collected from the 48-well plates and examined for their p24 antigen content using the HIV-1 p24 ELISA kit (NEN, Brussels, Belgium). Measurement of the cytotoxicity of the compound for both latently HIV-1-infected OM-10.1 and U1 cell lines in the 96-well plates was based on the 3-(4,5-dimethylthiazol-2-yl)-2,5-diphenyltetrazolium bromide (MTT) cell viability staining method as described previously [30]. For the antiviral activity assay in M/M, 24-well plates seeded with 150,000 cells per cup were treated with various concentrations of compound and infected with hundred 50% tissue culture infectious doses of HIV-1(BaL)/ml. After a 5-day incubation period, culture medium was replaced by fresh complete medium containing the appropriate compound concentration

and the M/M were then cultured for an additional 8 days. Supernatants were finally collected for assessment of virus production by analysis of HIV-1 p24 antigen (NEN, Brussels, Belgium).

2.4. Transactivation assays

Transactivation studies in HL_{tat} and $Jurkat_{tat}$ cells were performed as described previously [34]. Briefly, the HeLa-derived HL_{tat} cells were transfected in 0.7 ml of medium with 8 μg pHIV-GFPemd or pCMV-GFPemd plasmid DNA by electroporation with an Easyject One electroporator (Cell one, Belgium) in a 4 mm cuvette at 200 V; 1650 μF and infinite R. The electroporated cells (70×10^3/well) were incubated in 96-well microtiter plates for 24 h in the presence of varying concentrations of the test compound. Then, medium was removed by gentle aspiration, and the monolayers were washed with PBS. Inhibition of transactivation was measured with the Fluorocount (Packard) by quantification of GFP reporter gene activity at 24 h after transfection. The 50% inhibitory concentration (IC_{50}) was calculated as the compound concentration that reduced GFP expression by 50%. Cytotoxicity of the test compound against the cells was determined in the same cell cultures by the 3-(4,5-dimethylthiazol-2-yl)-2,5-diphenyltetrazolium bromide method. The experiments to determine the IC_{50} and CC_{50} values of the test compounds were performed in quadruplicate.

For $Jurkat_{tat}$ transfection, 30×10^6 cells were resuspended in 400 μl of medium together with 40 μg of pHIV-GFPemd or pCMV-GFPemd plasmid DNA and electroporated in a 4 mm cuvette at 250 V, 1050 μF and infinite R. Then, electroporated cells were resuspended in 2.5 ml of fresh medium and 100 μl of the obtained cell suspension was transferred to 96-well plates containing varying concentrations of the test compound and subsequently incubated for 24 h.

2.5. Preparation of nuclear extracts and electrophoretic mobility shift assay (EMSA)

Nuclear extracts were prepared from 10^7 latently HIV-1-infected OM-10.1 or U1 cells. Cells were washed in ice-cold phosphate-buffered saline (PBS, pH 7.4) and resuspended in 400 μl of ice-cold hypotonic buffer containing 10 mM HEPES (pH 7.9), 50 mM KCl, 2 mM $MgCl_2$, 1 mM DTT plus the EDTA-free protease inhibitor mixture (Roche Molecular Biochemicals). Following a 15 min incubation on ice, 25 μl of a 10% Nonidet P-40 solution was added. Nuclei were then pelleted by centrifugation at $10{,}000 \times g$, washed with the hypotonic buffer and resuspended in 40 μl ice-cold high-salt extraction buffer containing 50 mM HEPES (pH 7.9), 500 mM NaCl, 10% glycerol, 2 mM $MgCl_2$, 1 mM DTT plus the EDTA-free protease inhibitor mixture. After the nuclear lysates were centrifuged, supernatants were collected for EMSA. The protein concentration in the supernatants were determined using the Bradford assay method (Bio-Rad).

The EMSA was based on the binding of nuclear NF-κB or recombinant NF-κB p50 (Promega) to a ^{32}P-labeled NF-κB consensus oligonucleotide (Promega). The NF-κB oligonucleotide was labeled according to the manufacturer's protocol and incubated for 30 min with 10 μg nuclear protein extract plus binding buffer (Promega). Following incubation, the sample was loaded on a 6% non-denaturing polyacrylamide gel in 0.5× Tris/boric acid/EDTA (TBE) buffer. Gel shifts were examined with a Phosphorimager (Molecular Dynamics, CA) and analyzed using OptiQuant acquisition and analysis software (Perkin-Elmer, CA).

2.6. Western Blotting and indirect immunofluorescence

Nuclear and cytoplasmic extracts from latently HIV-1-infected OM-10.1 or U1 cells were prepared as described for EMSA. The protein concentration in the nuclear extracts was determined using the Bradford assay method. The protein concentration in the cytoplasmic extracts was determined using the BCA protein assay (Pierce).

For western blot detection, protein extracts were separated on 4–12% Novex Bis-Tris gels purchased from Invitrogen (Merelbeke, Belgium). The proteins were transferred onto polyvinylidene difluoride membranes (Amersham Biosciences). The membrane was incubated overnight at 4 °C for blocking in PBS containing 5% skim milk. After having been washed three times with 0.1% Tween 20 in PBS, the membrane was incubated for 1 h at room temperature with antibodies. The rabbit polyclonal anti-IκBα antibody and the mouse monoclonal anti-NF-κB antibody were both purchased from Santa Cruz Biotechnology. After three more washes with the PBS-Tween 20 buffer, the membrane was incubated for 1 h at room temperature with secondary horseradish peroxidase (HRP)-conjugated antibodies (Santa Cruz, CA). Detection was carried out using ECL Plus chemiluminescent horseradish peroxidase substrate (Amersham Biosciences).

Indirect immunofluorescent detection of NF-κB was performed on growing cells in LabTek II glass chamber slides (VWR International). Cells were fixed by incubation with 4% formaldehyde in PBS for 10 min, washed with PBS and permeabilized with ice-cold methanol. The cells were then blocked in PBS containing 10% FCS and 20 mM ammonium chloride for 30 min and incubated with monoclonal anti-NF-κB antibodies (used at a dilution 1:200), followed by Alexa-488-conjugated goat anti-mouse antibody (Molecular Probes, Leiden, The Netherlands). After three final washes with PBS-FCS buffer, the cells were photographed through a Zeiss Axiovert 40 CFL inverted microscope with LD A-Plan 20×/0.30 objective using a Canon Powershot G5 camera.

2.7. Measurement of intracellular oxidative stress

Intracellular oxidative stress was measured using the oxidant-sensitive fluorescent probe 2′,7′-dichlorofluorescein diacetate (DCFH-DA) (Molecular Probes, Leiden, The Netherlands). Cells were seeded at a density of 10^6 cells in growth medium supplemented with 10 μM DCFH-DA for 15 min. Next, various concentrations of JPL-32 were added to the cell suspension for another 15 min followed by exposure to 50 μM hydrogen peroxide (H_2O_2) solution for a final 15 min incubation period. After 45 min, cells were washed in PBS and seeded in a 96-well plate at a density of 2×10^5 cells/well. DCF fluorescence (excitation, 488 nm; emission, 520 nm) was imaged on a Zeiss Axiovert 40 CFL inverted microscope and quantified with the Fluorocount.

2.8. Measurement of apoptosis

2.8.1. DAPI staining

Jurkat$_{tat}$ cells were seeded into a 48-well plate at a concentration of 10^5 cells/well and pretreated with 10 μg/ml JPL-32 for 4 h. After having been washed with cold PBS, cells were transferred in LabTek II glass chamber slides and fixed by incubation with 3% formaldehyde in PBS for 30 min. Next, cells were permeabilized with 0.1% Triton X-100 in PBS for 10 min, washed three times with PBS and stained with 10 ng/ml DAPI (Molecular Probes, Leiden, The Netherlands) for 10 min. After three final washes with PBS, the cells were photographed using a Zeiss Axiovert 40 CFL inverted microscope.

2.8.2. Flow cytometric analysis of Annexin V binding

Jurkat$_{tat}$ cells were seeded into a 24-well plate at a concentration of 10^6 cells/well and were pretreated with various concentrations of the test compound in the presence or absence of 40 ng/ml FasL (R&D Systems). After an incubation period of 15 h, cells were washed in cold PBS and incubated

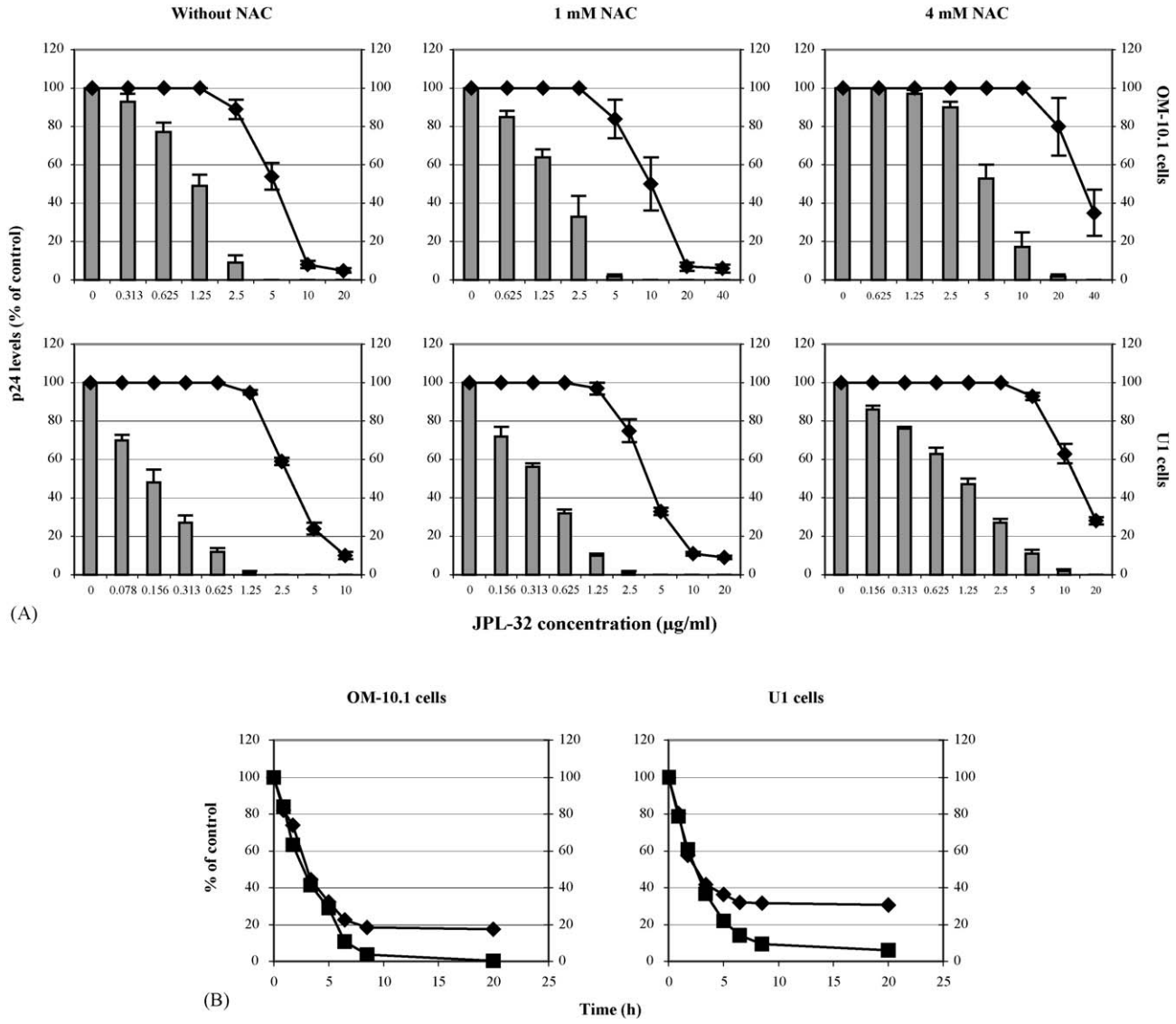

Fig. 2 – Inhibitory effect of JPL-32 with or without NAC supplementation on TNF-α-induced expression of HIV-1 in OM-10.1 and U1 cells. (A) The latently HIV-infected OM-10.1 and U1 cells were incubated with various concentrations of JPL-32 in the presence of 0, 1 and 4 mM NAC for 2 h, stimulated with 1 ng/ml TNF-α and further incubated for 48 h. Supernatants were then collected for p24 antigen quantification and the p24 levels are expressed as the percent of control (no compound). Cell cultures were examined for cell viability using the MTT method (◆). All experiments were carried out in quadruplicate, and results are presented as mean values with standard deviations. (B) Time-of-addition experiment with 4 mM NAC in OM-10.1 and U1 cell cultures treated with, respectively, 2.5 and 1.25 μg/ml JPL-32 for antiviral activity determination (■) and, respectively, 20 and 10 μg/ml JPL-32 for cytotoxicity assessment (◆). At $t = 0$, TNF-α-induced expression of HIV-1 was initiated in both cell lines in the presence of JPL-32. Following TNF-α stimulation, NAC was added at different points in time (0–20 h) and further incubated till 48 h post-stimulation. After this 2 day incubation period, p24 levels were assessed in the supernatants and expressed as the percent of control (■) and cell viability was examined using the MTT method (◆).

for 15 min with Annexin-V-Fluos reagent (Roche Diagnostics Belgium) in the dark. After this incubation period, cells were washed in cold PBS and resuspended in 500 μl 1% formaldehyde in PBS. Samples were analyzed on a FACSCalibur flow cytometer (BD Biosciences, San Jose, CA) using Cell Quest software (BD Biosciences) for data analysis.

2.8.3. *Quantitative caspase-3 assay*

Human active caspase-3 was quantified in Jurkat$_{tat}$ cell extracts using the caspase-3 Quantikine ELISA from R&D Systems. Briefly, Jurkat$_{tat}$ cells (2×10^6 cells/well) were seeded into a 24-well plate with various concentrations of the test compound all or not supplemented with 40 ng/ml FasL (R&D Systems). After 4 h incubation, 2 μl of 5 mM biotin-ZVKD-fmk inhibitor was added and incubated for another hour. Next, cells were centrifuged, washed in PBS and lysed with an extraction buffer (R&D Systems) containing the EDTA-free protease inhibitor mixture (Roche Molecular Biochemicals). After an overnight lysing period at 4 °C, samples were diluted 10-fold with a kit diluent and immediately assayed with the caspase-3 ELISA.

2.9. *Intracellular GSH measurement*

We measured intracellular contents of GSH using the Bioxytech GSH-412 assay (Oxis International) and the Bioxytech GSH-400 patented method (Oxis International) [13]. Briefly, 2×10^6 latently HIV-1-infected OM-10.1 or U1 cells were incubated with various concentrations of JPL-32 for different time periods. Then, the cells were washed with PBS, resuspended in 100 μl PBS and stored at −80 °C. After thawing, cells were vortexed and supplemented with 200 μl 5% metaphosphoric acid solution (Sigma). Samples were again vortexed and centrifuged at 1000 × *g* for 10 min. Supernatants were then ready for GSH determination using both Bioxytech assays. The Bioxytech GSH-412 assay uses an enzymatic cycling reaction with the Ellman's Reagent (5,5′-dithiobis-2-nitrobenzoic acid or DTNB), which reacts with GSH to form a spectrophotometrically detectable product at 412 nm. The Bioxytech GSH-400 assay uses 4-chloro-1-methyl-7-trifluromethyl-quinolinium methyl-sulfate that reacts with all mercaptans (RSH) and transforms them into chromophoric

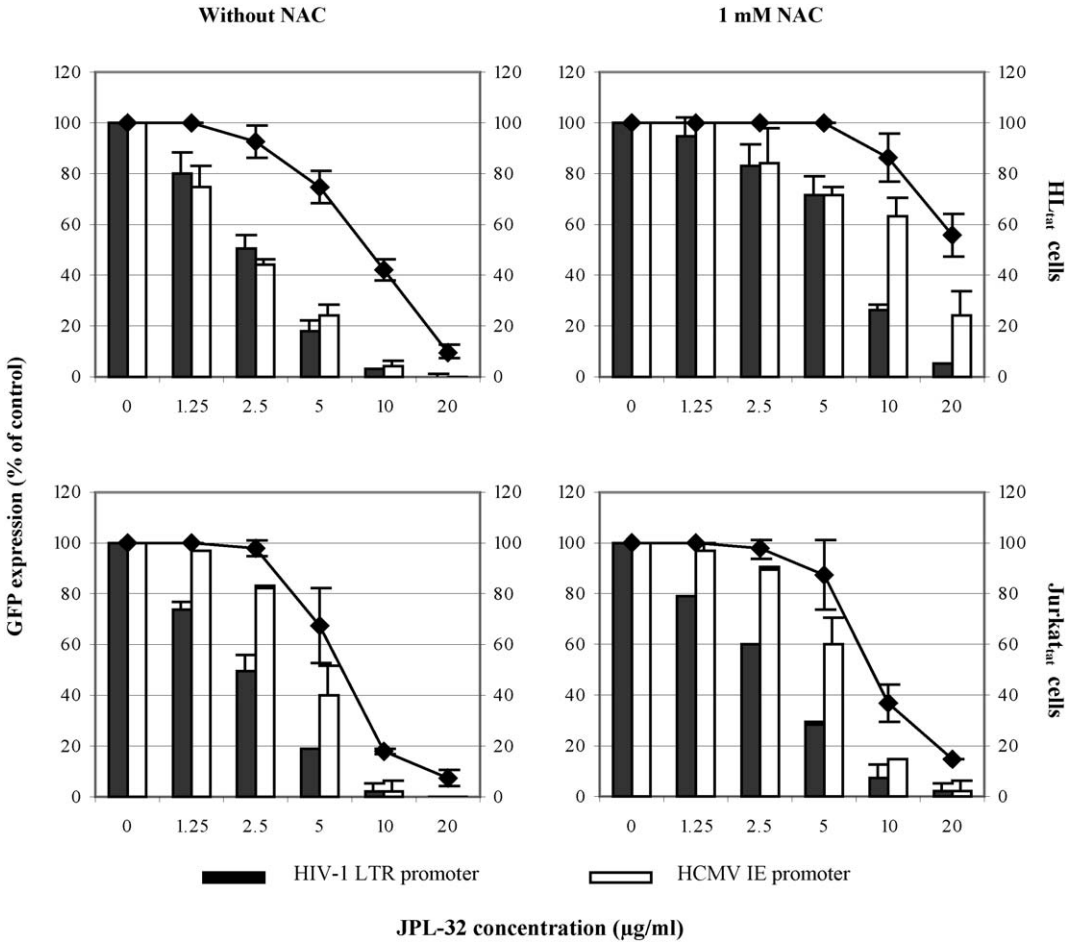

Fig. 3 – Inhibitory effect of JPL-32 with or without NAC supplementation on GFP transactivation. Constructs using the GFP reporter gene transcribed from the HIV-1 LTR (black bars) and the HCMV IE (white bars) promoter were used to investigate the effect of JPL-32 on the transactivation process. HL$_{tat}$ and Jurkat$_{tat}$ cells were transfected with the GFP-expressing constructs and incubated with different concentrations of JPL-32 in the presence or absence of 1 mM NAC for 24 h. Quantification of GFP production was measured with the Fluorocount and expressed as the percent of control. Cell viability was determined in the same cell cultures by the MTT method (◆). All experiments were carried out in quadruplicate, and results are presented as mean values with standard deviation.

thiones under alkaline conditions which have a maximal absorbance wavelength at 400 nm.

3. Results

3.1. *Inhibition of HIV-1 replication in monocytes/macrophages*

The pyridine *N*-oxide JPL-32 was examined for its inhibitory effect on acutely HIV-1-infected human primary monocytes/macrophages (M/M) as well as on latently HIV-1-infected promyelocytic cells (OM-10.1) and latently HIV-1-infected promonocytic cells (U1). Upon infection of M/M with the HIV-1 (BaL) strain, JPL-32 proved inhibitory at an EC_{50} value (or compound concentration required to inhibit HIV-1 p24 production by 50%) of 0.24 μg/ml (data not shown). Treatment of latently HIV-1-infected OM-10.1 and U1 cell lines with TNF-α in the absence of JPL-32 caused a dramatic (~1000-fold) increase in HIV-1 expression, which was set as hundred percent (Fig. 2A). In the presence of varying concentrations of JPL-32 a dose-dependent inhibition of HIV p24 production was observed in both cell lines. Remarkably, addition of NAC, a well-known antioxidant used to replenish intracellular GSH levels, to the culture medium revealed a reversing effect on the antiviral activity of JPL-32 in both OM-10.1 and U1 cell lines (Fig. 2A). In addition, not only the antiviral activity but also the cytotoxicity of JPL-32 decreased in a NAC dose-dependent way in both cell lines. However, the selectivity index (CC_{50}/EC_{50}) of JPL-32 remained similar in the presence, or in the absence, of NAC at a concentration up to 4 mM.

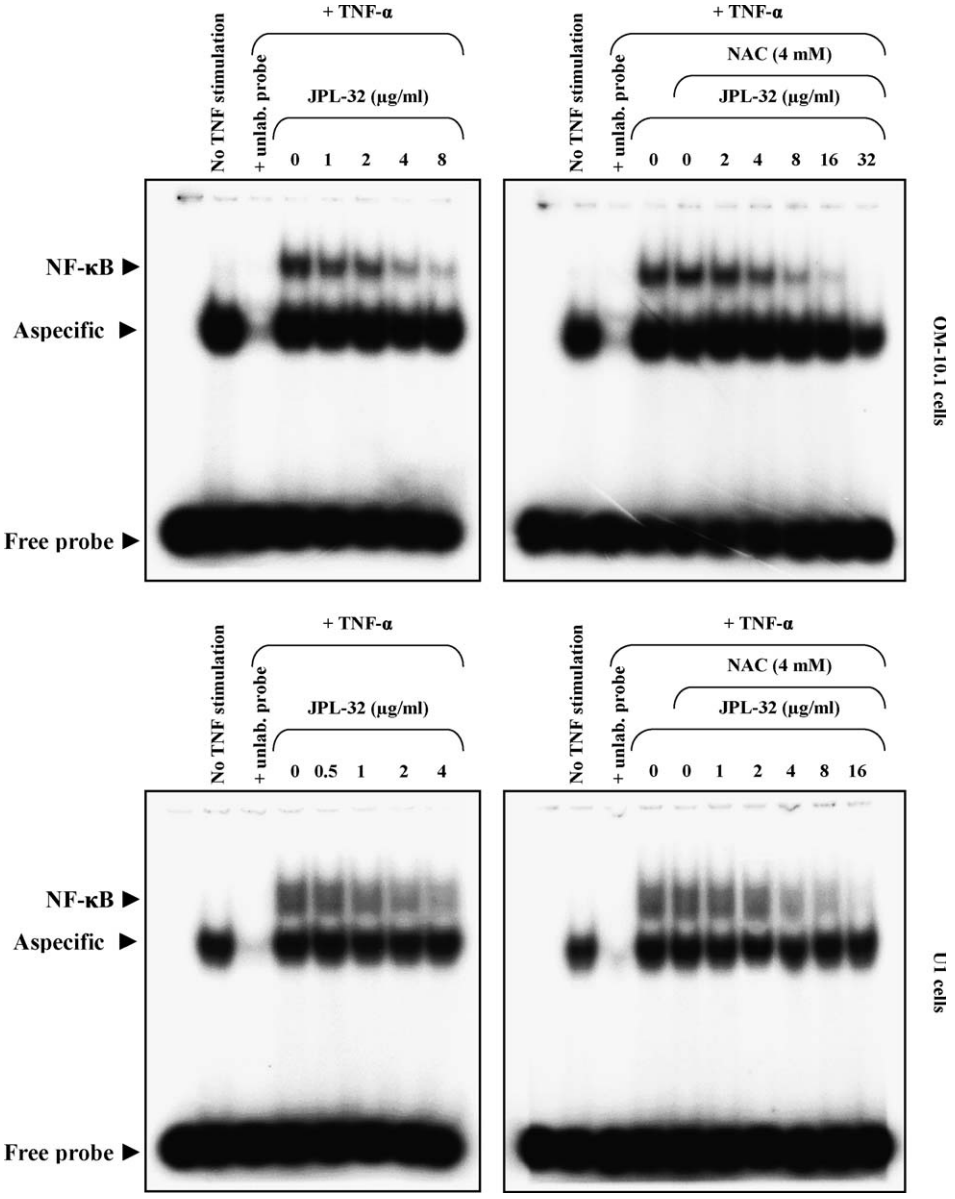

Fig. 4 – Inhibition of TNF-α-induced DNA binding of nuclear NF-κB by JPL-32 with or without NAC supplementation. OM-10.1 and U1 cells were cultured with various concentrations of JPL-32 in the presence and absence of 4 mM NAC for 1 h. Following a 30 min TNF-α stimulation, nuclear extracts were prepared and analyzed for NF-κB binding by EMSA.

In order to have a notion for how long we can postpone the supplementation of NAC without affecting cell viability and to have an idea for how long NAC can reverse the antiviral activity of JPL-32, we performed a time-of-addition experiment with 4 mM NAC on both OM-10.1 and U1 cell lines (Fig. 2B). As shown in Fig. 2B, the reversing effect of NAC, not only on cytotoxicity but also on the antiviral activity rapidly decreased when the addition of NAC was delayed after JPL-32 exposure. After 5 h, addition of NAC was no longer able to significantly reverse the cytotoxicity or the antiviral activity of JPL-32.

3.2. *Inhibition of GFP transactivation*

Since JPL-32 is able to inhibit the replication of HIV-1 and CMV in cell culture and interacts at a post-integrational level in the replication cycle of HIV, the effect of JPL-32 on the transactivation of the GFP reporter gene mediated from the HIV-1 LTR and the human CMV IE promoter was investigated. As shown in Fig. 3, JPL-32 inhibited the Tat-mediated GFP gene expression from the HIV-1 LTR promoter in HL_{tat} cells in a dose-dependent manner. When transfection was carried out with the other GFP-expressing construct, a similar dose-dependent decrease could be observed. Also in this experiment, addition of 1 mM NAC caused a dramatic decrease in cytotoxicity as well as a marked reversal of the inhibitory effect of JPL-32 on GFP gene expression in HL_{tat} cells. Transfection of $Jurkat_{tat}$ cells with the GFP-expressing constructs revealed a similar inhibitory effect of JPL-32 on gene expression as observed in HL_{tat} cells (Fig. 3). Supplementation of 1 mM NAC was also able to reverse the effects of JPL-32 in $Jurkat_{tat}$ cells, but to a lesser extent compared with HL_{tat} cells.

3.3. *Inhibition of nuclear NF-κB DNA binding*

As we clearly observed an inhibitory effect of JPL-32 on viral transactivation that could be reversed by NAC, it would be interesting to investigate the potential role of the redox-sensitive NF-κB transcription factor in the inhibitory activity of JPL-32. OM-10.1 and U1 cells were cultured with various concentrations of JPL-32, stimulated by TNF-α, and nuclear extracts were examined for binding to the ^{32}P-labeled NF-κB oligonucleotide in the EMSA assay. As shown in Fig. 4, JPL-32 inhibited the DNA binding of nuclear NF-κB in a dose-dependent way. When TNF-α-stimulated OM-10.1 cells were treated with 4 and 8 μg/ml JPL-32, NF-κB DNA binding was dramatically reduced. This inhibitory effect of JPL-32 could be partially neutralized by the addition of 4 mM NAC to the OM-10.1 cell cultures. In order to regain the inhibitory potency of JPL-32 with 4 mM NAC, the concentration of JPL-32 had to be increased to 8 and 16 μg/ml, respectively (Fig. 4). It should be noted that the cytotoxic effects of JPL-32 at 16 μg/ml were also partially reversed by NAC. A similar observation was found when nuclear extracts of TNF-α-stimulated U1 cells treated with JPL-32 were analyzed for NF-κB DNA binding activity. In order to determine the specificity of NF-κB for its DNA binding sites, preincubation with the unlabeled NF-κB oligonucleotide was performed.

3.4. *Effect of JPL-32 on IκBα degradation and regeneration*

The dose-dependent inhibition of nuclear NF-κB DNA binding by JPL-32 may be attributed to an inhibition of the degradation of IκBα which was investigated by western blotting. TNF-α induces phosphorylation and subsequent proteasome-mediated degradation of IκBα to release NF-κB from the inactive complex. As shown in Fig. 5, the TNF-α-induced degradation of IκBα was completed after 10 min in OM-10.1 and U1 cells. Thereafter, IκBα synthesis was resumed by NF-κB binding to the IκBα promoter [37]. This regeneration of IκBα was completed within 60 min upon TNF-α stimulation of both cell lines (Fig. 5). At a concentration of 8 and 4 μg/ml, respectively, JPL-32 did not inhibit the release and subsequent degradation of IκBα in OM-10.1 and U1 cells. However, at these concentrations of JPL-32, IκBα was much less re-synthesized after 60 min, as shown in Fig. 5. This observation is in agreement with the EMSA data which indicate that inhibition of NF-κB activity inhibits the regeneration of IκBα mRNA. Upon supplementation of 4 mM NAC, similar IκBα regeneration inhibitory effects of JPL-32 were observed in both cell lines, though at a higher concentration. Thus, JPL-32 did not inhibit the degradation of IκBα at a concentration that inhibited the activation of NF-κB.

3.5. *Nuclear translocation of NF-κB*

In order to investigate whether NF-κB was translocated to the nucleus upon release from IκBα, immunofluorescent detection of p65 was conducted in HL_{tat} cells, COS-7 cells and OM-10.1 cells. As shown in Fig. 6A, NF-κB was present in the cytoplasm of cells that were not exposed to TNF-α. However, a similar nuclear staining was microscopically observed in JPL-32-treated and untreated cells after TNF-α stimulation. Surprisingly, nuclear translocation of NF-κB was even remarkably enhanced in HL_{tat} cells upon JPL-32 exposure. Western blot analysis of nuclear fractions of OM-10.1 cells with p65-specific antibodies showed the presence of NF-κB in the nucleus,

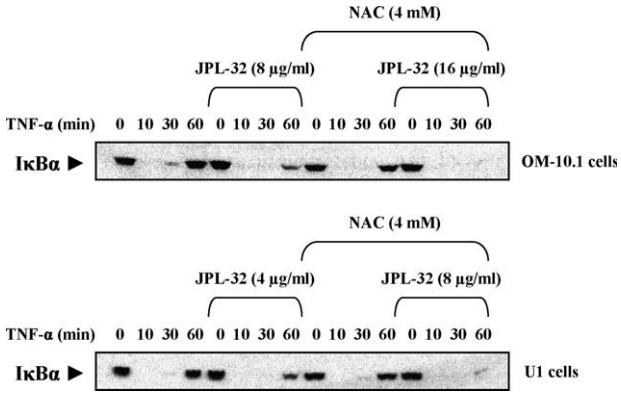

Fig. 5 – Effect of JPL-32 on TNF-α-induced release and subsequent degradation of IκBα from NF-κB. OM-10.1 and U1 cells were treated with TNF-α as such or in the presence of JPL-32 with or without NAC for the indicated time periods (in min). The cytoplasmic lysates were prepared and fractionated on 4–12% Novex Bis-Tris gels and analyzed for the presence of IκBα.

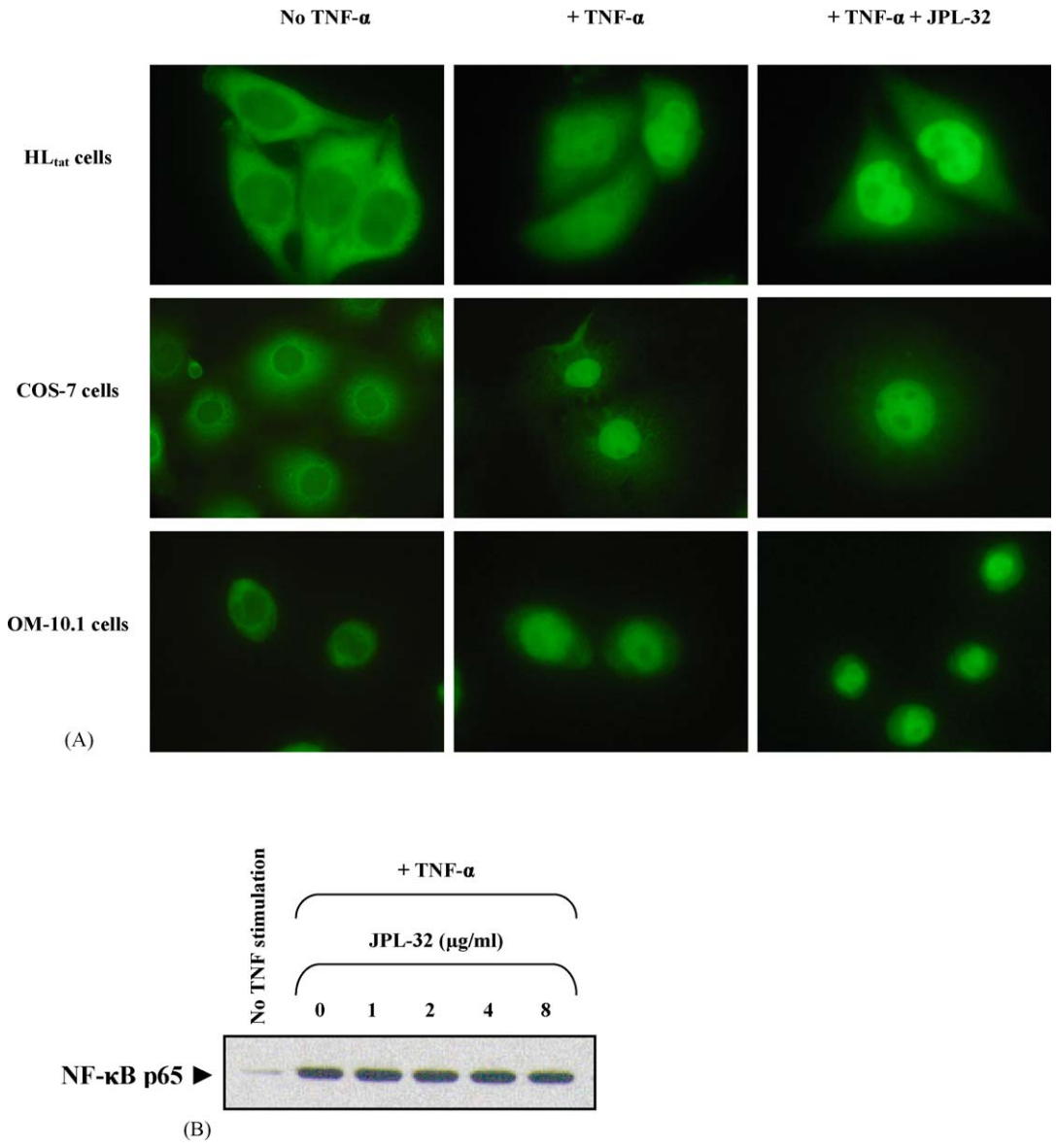

Fig. 6 – Effect of JPL-32 on TNF-α-induced nuclear translocation of NF-κB. (A) immunofluorescence analysis. HL_{tat}, COS-7 and OM-10.1 cells were treated with TNF-α for 30 min in the presence or absence of JPL-32. Then, the cells were fixed, permeabilized, and examined by fluorescence microscopy. (B) Western blot analysis of nuclear NF-κB in OM-10.1 cells. Cells were cultured with various concentrations of JPL-32 and stimulated with TNF-α for 30 min. The nuclear fractions were fractionated on 4–12% Novex Bis-Tris gels and analyzed for NF-κB.

which is consistent with the lack of inhibition of NF-κB translocation by JPL-32 (Fig. 6B).

3.6. *Oxidoreductive modulation of NF-κB upon JPL-32 exposure*

In addition to the inhibitory effect of JPL-32 on the DNA binding of nuclear NF-κB from JPL-32-treated OM-10.1 cells, we examined the effect of an excess of reducing agents to the nuclear extracts. As shown in Fig. 7, we found that the inhibition caused by JPL-32 could be reversed by treatment of nuclear extracts from JPL-32-treated OM-10.1 cells with reducing agents DTT and β-mercaptoethanol, strongly suggesting a thiol-dependent modification of NF-κB by JPL-32.

3.7. *Effect of JPL-32 on the direct binding of NF-κB to the κB DNA binding sites*

In order to investigate the direct effect of JPL-32 on DNA binding of NF-κB, the compound was added after the nuclear extract preparation of TNF-α-stimulated OM-10.1 cells. As shown in Fig. 8A, JPL-32 caused a dramatic inhibition of the NF-κB DNA binding activity at a concentration of 50 and 100 μg/ml. Addition of JPL-32 at 10 and 20 μg/ml showed only a moderate inhibition of the binding of NF-κB to its DNA binding sites. In addition, when JPL-32 was analyzed for its effect on the p50 subunit of recombinant NF-κB, an identical dramatic inhibition of the NF-κB DNA binding activity was observed at a concentration of 50 and 100 μg/ml (Fig. 8B).

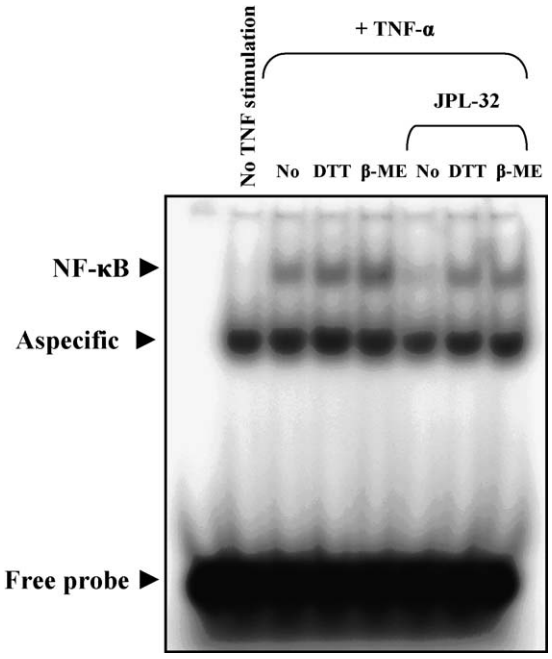

Fig. 7 – Oxidoreductive modulation of the DNA binding activity of nuclear NF-κB. OM-10.1 cells were cultured for 1 h with 8 μg/ml JPL-32. Following a 30 min. TNF-α stimulation, nuclear extracts were treated with 10 mM DTT or 1% β-mercaptoethanol (β-ME) for 1 h and analyzed for NF-κB binding by EMSA.

Addition of an excess of β-mercaptoethanol to the JPL-32-treated samples reversed the inhibition of NF-κB p50 binding to DNA caused by JPL-32.

3.8. *Induction of intracellular oxidative stress*

Generation of oxidative stress by H_2O_2 leads to activation of NF-κB and, subsequently, to the stimulation of HIV-1 expression [12,23]. Treatment of OM-10.1 cells with 50 μM H_2O_2 caused a (~100-fold) increase in HIV-1 expression (data not shown). In order to analyze and quantify the oxidative stress caused by the addition of 50 μM H_2O_2 to OM-10.1 cells, addition of DCFH-DA caused a more than eight-fold increase in DCF fluorescence compared to untreated OM-10.1 cells (Fig. 9A and B). When JPL-32 was added to the H_2O_2-treated cell cultures, a dose-dependent inhibition of HIV p24 production was found (data not shown). The inhibitory effect of JPL-32 on HIV-1 expression in OM-10.1 cells after stimulation with H_2O_2 was similar as noted for TNF-α stimulation (Fig. 2A). Although HIV-1 expression was inhibited, JPL-32 increased the intracellular oxidative stress within OM-10.1 cells in a concentration-dependent way (Fig. 9A and B). The induction of oxidative stress caused by JPL-32 in the presence of H_2O_2 was as profound as in the absence of H_2O_2 (Fig. 9B).

3.9. *Induction of apoptosis*

JPL-32 induced apoptotic morphology in $Jurkat_{tat}$ cells, as shown in Fig. 10A. Nuclear DNA fragmentation became clearly visible 4 h after treatement with 10 μg/ml JPL-32. When the

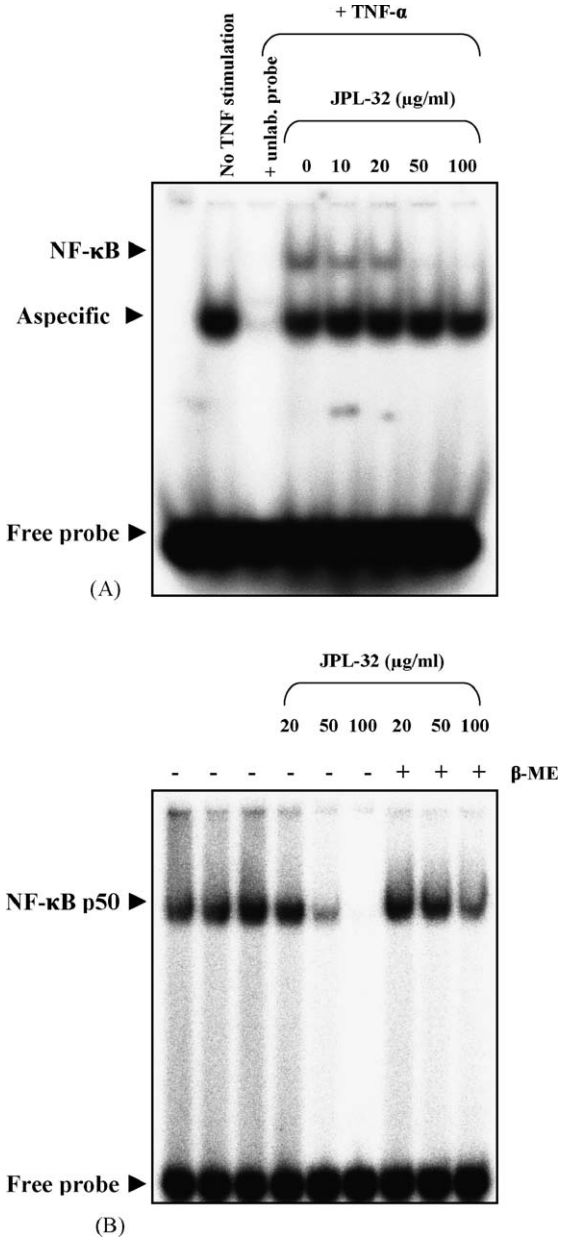

Fig. 8 – Effect of JPL-32 on the direct DNA binding of NF-κB. Nuclear extracts from TNF-α-stimulated OM-10.1 cells (A) and recombinant NF-κB p50 (B) were treated with various concentrations of JPL-32 in the presence or absence of 1% β-mercaptoethanol (β-ME) and analyzed for binding to the ^{32}P-labeled NF-κB oligonucleotide in the EMSA assay. In order to exclude the effect of the solvent DMSO, which is present in the JPL-32 stock solution, the first three lanes of (B) contains equal amounts of DMSO compared to the following three lanes, containing JPL-32, and the last three lanes, that contain JPL-32 and 1% β-ME.

externalization of phosphatidylserine as a marker for apoptotic cell death was examined upon JPL-32 exposure, a dose-dependent increase of annexin-V-FITC binding was observed by flow cytometry (Fig. 10B). At a concentration of 2.5 μg/ml, only a few cells became apoptotic while a concentration of 10 μg/ml JPL-32 pushed nearly all cells into an apoptotic state.

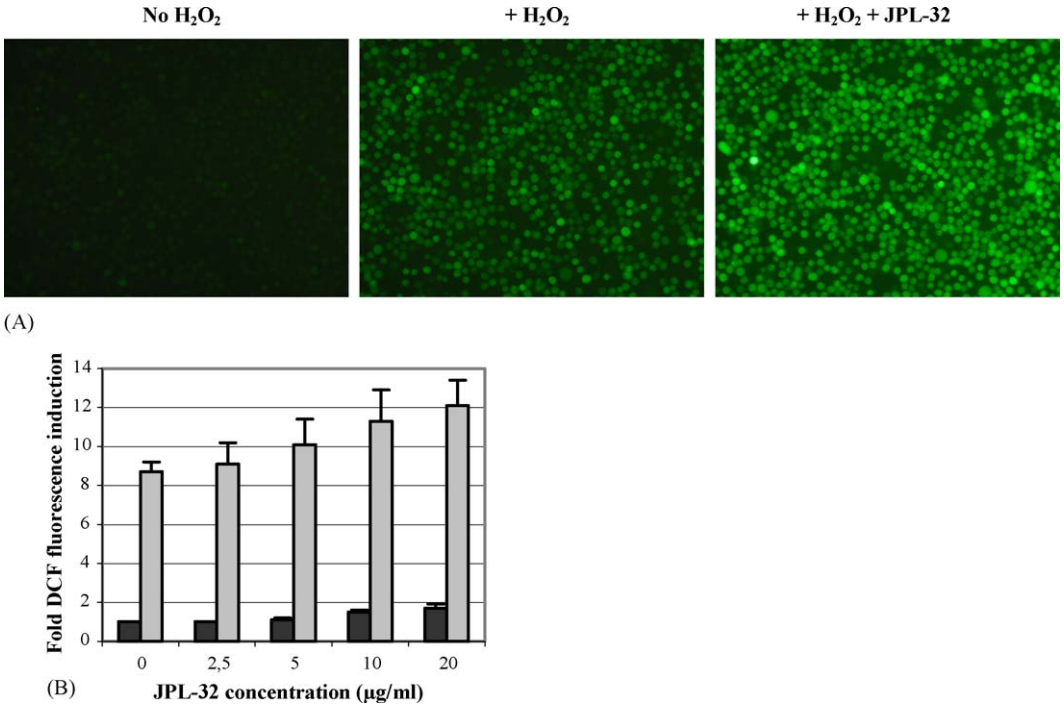

Fig. 9 – Determination of intracellular oxidative stress in OM-10.1 cells. Cells were treated with 10 μM DCFH-DA for 15 min. Then, various concentrations of JPL-32 were added to the cell suspension for another 15 min followed by the absence (dark grey bars) or presence of 50 μM H_2O_2 (light grey bars) for a final 15 min. After this 45 min incubation period, cells were washed in PBS and seeded in a 96-well plate at a density of 2×10^5 cells/well. DCF fluorescence was imaged by fluorescence microscopy (A) and measured with the Fluorocount (B).

Determination of active caspase-3 revealed consistent results with lack of active caspase-3 at a concentration of 2.5 μg/ml JPL-32 but maximal caspase-3 activity upon 10–20 μg/ml JPL-32 exposure (Fig. 10C). These results are in full agreement with the previous cytotoxic data found for JPL-32 in $Jurkat_{tat}$ cells using the MTT method (Fig. 3).

Next, the effect of JPL-32 on the apoptotic sensitivity of $Jurkat_{tat}$ cells to FasL was investigated. In the absence of JPL-32, FasL induced about 30% of the cells into apoptosis while the active caspase-3 activity increased five-fold. When 2.5 μg/ml JPL-32 was added, the FasL-induced apoptosis was dramatically increased with over 60% of the cells going into apoptosis. Not only annexin-V-FITC binding increased but also caspase-3 activity was increased another two-fold upon JPL-32 (2.5 μg/ml) exposure. Thus, JPL-32 increased apoptotic sensitivity to FasL in $Jurkat_{tat}$ cells.

3.10. *Effect of JPL-32 on the intracellular GSH levels*

In order to further investigate the redox status of OM-10.1 and U1 cells upon JPL-32 exposure, intracellular GSH levels were measured using two different methods. Both GSH quantification methods produced identical results. GSH levels in OM-10.1 and U1 cells were significantly increased after 4 h treatment with JPL-32 (Fig. 11A). Initially, GSH levels dropped slightly but this effect was immediately reversed, and GSH levels increased with another 40% of control after 12 h of JPL-32 treatment in both cell lines. Then, OM-10.1 and U1 cells were incubated with various concentrations of JPL-32 and analyzed for their intracellular GSH content. As shown in Fig. 11B, a dose-dependent induction of GSH in OM-10.1 and U1 cells was found. To investigate whether this GSH increase is caused by the intracellular reduction of GSSG or whether it is due to newly synthesized GSH by γ-glutamylcysteine synthetase, we added buthionine sulfoximine (BSO), an irreversible inhibitor of γ-glutamylcysteine synthetase, to the cell cultures. In the absence of JPL-32, intracellular GSH levels dropped to more than 80% of control (Fig. 11C). When JPL-32 was added to the cell cultures in the absence of BSO, intracellular GSH increased to approximately 140% of the control, as found previously (Fig. 11A). When JPL-32 was added in the presence of BSO, no GSH induction was observed, although a further, only slight, drop of GSH content was found, indicating the involvement of newly synthesized GSH upon JPL-32 exposure.

4. Discussion

The present study reveales the underlying molecular mechanism that explain the antiviral properties of pyridine N-oxide derivatives [3,4,35,36]. We have demonstrated that the prototype JPL-32 not only inhibits HIV-1 replication in acutely HIV-1-infected M/M cells, but that JPL-32 is also an efficient inhibitor of TNF-α-induced HIV-1 expression in latently HIV-1-infected OM-10.1 and U1 cell lines. These findings show that JPL-32 is able to control HIV-1 replication in both acutely infected cells and chronically infected cells, which makes the

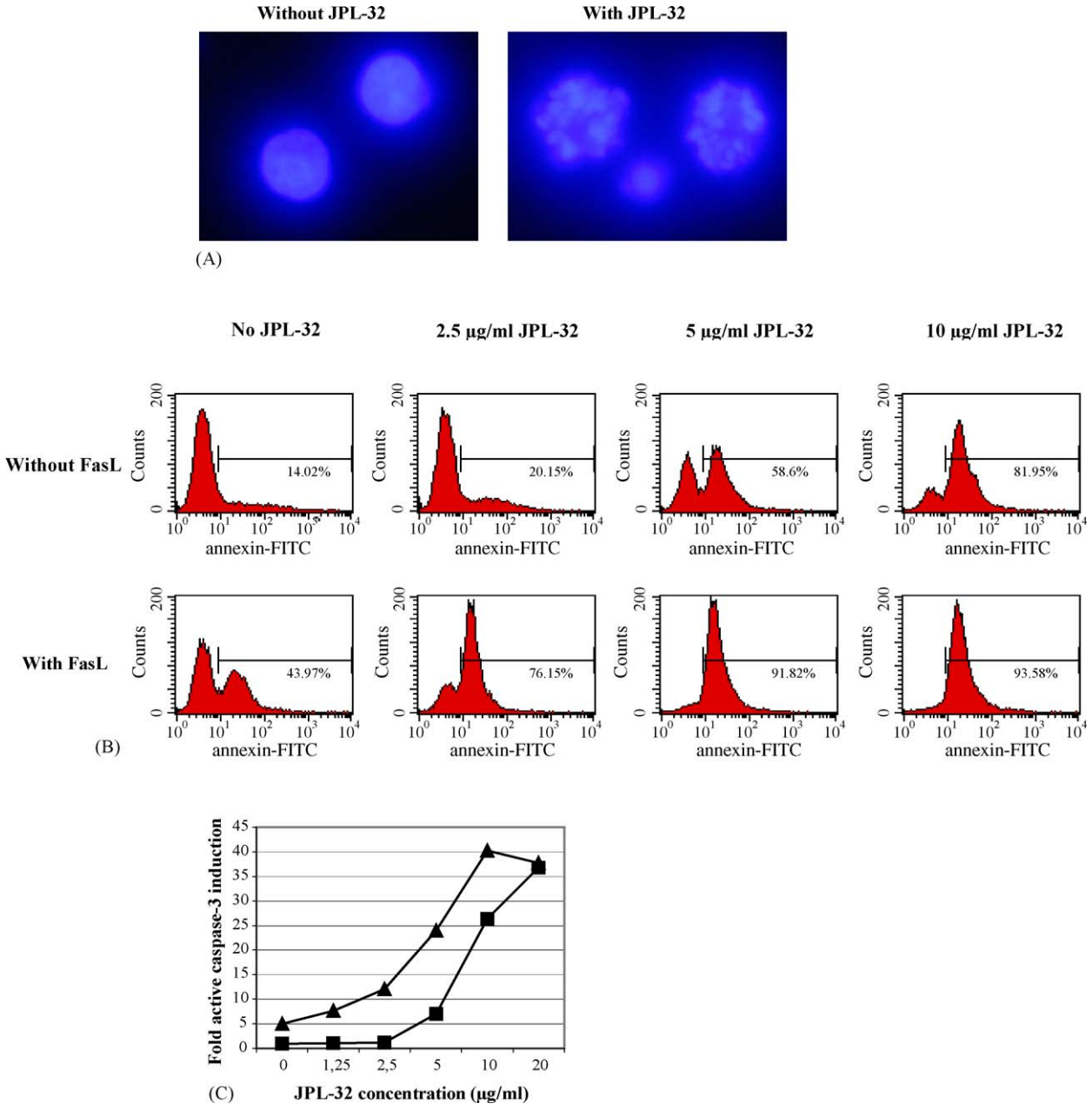

Fig. 10 – Induction of apoptosis by JPL-32. (A) Jurkat$_{tat}$ cells were treated with 10 μg/ml JPL-32 for 4 h. Then, the cells were fixed, permeabilized, stained with DAPI and examined by fluorescence microscopy. (B) Jurkat$_{tat}$ cells were cultured for 15 h with various concentrations of JPL-32 in the presence and absence of 40 ng/ml FasL. Following incubation, cells were incubated for 10 min. with Annexin-V-Fluos reagent and analyzed with a flow cytometer. (C) Jurkat$_{tat}$ cells were treated with various concentrations of JPL-32 in the presence (▲) or absence (■) of 40 ng/ml FasL for 5 h and assayed for intracellular active caspase-3 by ELISA.

compound very attractive in anti-HIV drug combination therapies. In this context, the compound could not only force the virus to remain in its dormant latent state, but could also result in a lower incidence of drug resistance as HIV transactivation requires the interplay of both viral and cellular components [1,10]. Remarkably, when NAC was added to the JPL-32-treated OM-10.1 and U1 cell cultures, not only the antiviral activity but also the cytotoxicity of JPL-32 decreased in a NAC dose-dependent way. A similar effect of NAC was observed for the inhibitory effect of JPL-32 on the GFP transactivation mediated from the HIV-1 LTR and the human CMV IE promoter. As we observed that the reversing effect of this antioxidant on both inhibitory activity and cytotoxicity of JPL-32 could only be sustained for a period of 5 h, the possible involvement of a redox-sensitive transcription factor appeared plausible. Indeed, when nuclear extracts of TNF-α-stimulated OM-10.1 and U1 cells cultured in the presence of JPL-32 were subjected to EMSA with a ^{32}P-labeled NF-κB oligonucleotide, a dose-dependent inhibition of DNA binding of nuclear NF-κB was found, which could be reversed by NAC.

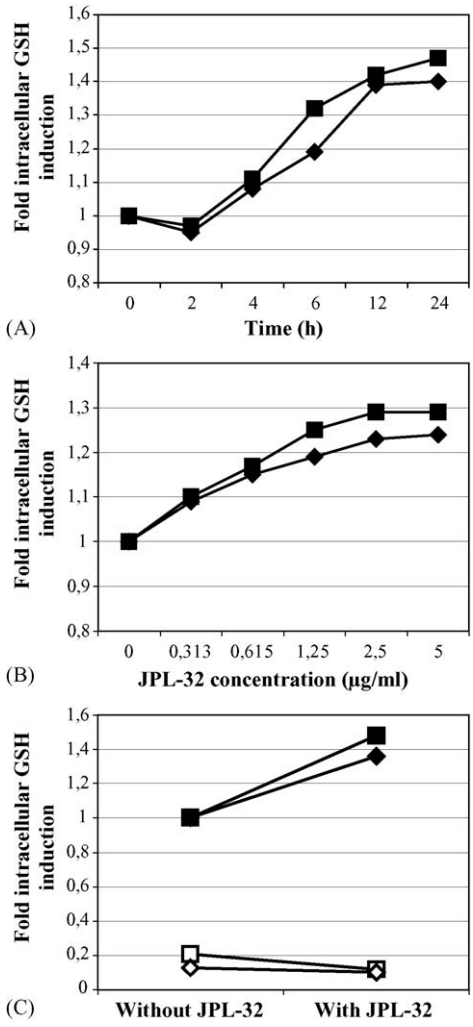

Fig. 11 – Induction of intracellular GSH levels by JPL-32 in OM-10.1 and U1 cells. (A) OM-10.1 (■) and U1 (◆) cells were cultured in the presence of respectively, 2.5 and 1.25 μg/ml JPL-32. After different periods, samples were taken and analyzed for intracellular GSH content by two different methods. (B) OM-10.1 (■) and U1 (◆) cells were treated with various concentrations of JPL-32 for 4 h. Following incubation, samples were subjected for intracellular GSH determination by the two different methods. (C) OM-10.1 (■ and □) and U1 (◆ and ◇) cells were cultured with respectively, 2.5 and 1.25 μg/ml JPL-32 in the presence (not filled) and absence (filled) of 200 μM buthionine sulfoximine (BSO). After an incubation period of 24 h, samples were taken and analyzed for intracellular GSH content by the Bioxytech GSH-400 method.

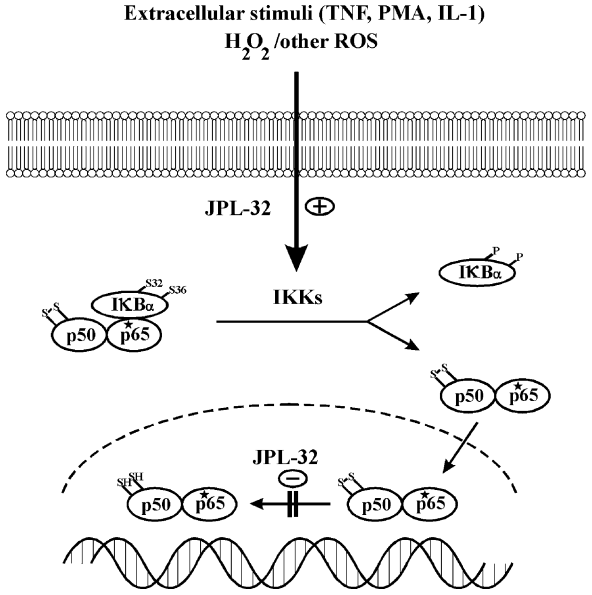

Fig. 12 – Redox regulation of NF-κB activation. Activation and nuclear translocation of NF-κB has been reported to occur under oxidative conditions and are stimulated by JPL-32, whereas the binding of NF-κB to the DNA promoter sequences has been shown to be dependent on reducing conditions which are blocked by JPL-32.

To gain more information on the exact inhibitory effect of JPL-32 on the NF-κB transduction pathway, the activation and nuclear translocation of NF-κB was investigated. We found that JPL-32 did not inhibit the release and subsequent degradation of IκBα in OM-10.1 and U1 cells. However, JPL-32 inhibited the regeneration of IκBα. This observation is in agreement with the EMSA data which prove that inhibition of NF-κB activation prevents the regeneration of IκBα. In other words, JPL-32 did not inhibit the degradation of IκBα at a concentration that inhibited the activation of NF-κB. When nuclear translocation of NF-κB was investigated, no inhibition could be observed upon JPL-32 exposure. Surprisingly, nuclear translocation of NF-κB was even remarkably enhanced in HL_{tat} cells upon JPL-32 treatment.

Having established NF-κB as a target of JPL-32 in EMSA and having confirmed its presence in the nuclear extracts of latently HIV-infected cells treated with JPL-32, we focussed on the mechanism of direct inactivation of NF-κB by JPL-32. Indeed, EMSA revealed that the inhibition of DNA binding of NF-κB in nuclear extracts from TNF-α-stimulated OM-10.1 cells cultured in the presence of JPL-32 could be reversed by the addition of reducing agents such as DTT or β-mercaptoethanol. This observation suggests a direct, reversible and thiol-dependent modification of NF-κB by JPL-32. We prove that JPL-32 was able to directly inhibit nuclear NF-κB DNA binding from TNF-α-stimulated OM-10.1 cells at a concentration of 50 μg/ml. In order to confirm this finding, the EMSA was repeated with the purified p50 subunit of recombinant NF-κB and provided the affirmative answer that JPL-32 modified directly the thiol groups in the p50 subunit of NF-κB at a concentration of 50 μg/ml. Addition of a reducing agent such as β-mercaptoethanol to the JPL-32-treated samples reversed the inhibition of NF-κB p50 binding to DNA caused by JPL-32 and proved the oxidative modulation of the NF-κB p50 DNA binding activity by JPL-32.

After having shown that JPL-32 acts as an oxidant and is able to oxidize the thiol groups in NF-κB, we analyzed the intracellular oxidative stress response upon JPL-32 exposure. We found that JPL-32 is able to increase oxidative stress within OM-10.1 cells in the absence, as well as in the presence of H_2O_2.

The finding that JPL-32 increases intracellular oxidative stress explains the inhibition of NF-κB p50 DNA binding, but also the enhanced nuclear translocation of NF-κB. Indeed, NF-κB is a redox-sensitive transcription factor tightly regulated by the intracellular redox status, which is maintained mainly by the ratio of reduced and oxidized GSH. Although NF-κB activation and nuclear translocation has been reported to occur under oxidative conditions, the binding of NF-κB to the DNA promoter sequences has been shown to be dependent on reducing conditions [15]. Therefore, it is not surprising that oxidants, such as JPL-32, enhance NF-κB activation but also impair DNA binding activity (Fig. 12).

Returning to the NAC effect upon JPL-32 exposure, it is now very obvious to explain the reversing effect of this antioxidant on the inhibitory activity of JPL-32. However, the decreased cytotoxicity of JPL-32 in the presence of NAC is still not very well understood. In order to clarify this reversing effect, we searched for the cause of cell death upon treatment of toxic JPL-32 concentrations. As we found that JPL-32 was able to induce apoptosis by phosphatidylserine externalization and increase active caspase-3 activity, we also observed an increased apoptotic sensitivity of Jurkat$_{tat}$ cells to FasL upon JPL-32 treatment. The fact that FasL sensitized Jurkat cells to apoptosis by the cleavage of NF-κB subunits [31] and that transfection of Jurkat cells with the NF-κB subunits confers resistance against FasL-mediated apoptosis [11,21], emphasizes our findings that inhibition of NF-κB can make the cells more susceptible to FasL-induced apoptosis. Since apoptosis is a redox-regulated cellular process (dependent on the presence of thiol groups) [32], blocking the anti-apoptotic transcription factor NF-κB [20,26,27,40] makes it easy to explain that apoptotic cell death is induced by JPL-32 and reversed by NAC.

It was shown that JPL-32 creates a pro-oxidant effect within the cell. Therefore, it should not be surprising that the intracellular redox status is altered upon JPL-32 exposure. As the redox state is mainly determined by the ratio GSH/GSSG, we measured the intracellular GSH levels upon JPL-32 treatment and found that GSH increased in OM-10.1 and U1 cells after 4 h treatment with JPL-32. Initially, GSH levels dropped slightly but this effect was immediately reversed, and GSH levels increased with another 40% of control after 12 h of JPL-32 treatment in both cell lines. In order to investigate the fact whether this GSH increase is caused by the intracellular reduction of GSSG or whether it is due to newly synthesized GSH by γ-glutamylcysteine synthetase, we added BSO, an irreversible inhibitor of γ-glutamylcysteine synthetase, to the cell cultures. When JPL-32 was added in the presence of BSO, no GSH induction was observed, though a further, only slight, drop of GSH content was found, which most likely indicates that the GSH increase by JPL-32 is caused by newly synthesized GSH. As it was previously reported that γ-glutamylcysteine synthetase expression is upregulated by oxidative stress [19], our findings of the effect of JPL-32 on the redox state are in agreement with these observations.

Taken together, we demonstrated that JPL-32 is an effective inhibitor of HIV in acutely and latently HIV-infected cells likely by oxidative modulation of the NF-κB p50 DNA binding activity. Additionally, JPL-32 creates a pro-oxidant effect within the cells and, by this, induces apoptosis and increases intracellular GSH levels. As JPL-32 has been proven to be an effective anti-HIV drug in vivo, further studies should now be warranted to investigate the potential of JPL-32 as an anti-inflammatory or anticancer drug.

Acknowledgments

These investigations were supported by grants from the European Commission (Credit No. QLRT 2000-00291, QLRT 2001-01311 and the René Descartes Prize 2001 No. HPAW-2002-90001), the ''Geconcerteerde Onderzoeksacties Vlaanderen'' (Project No. GOA-2005/19) and the ''Fonds voor Wetenschappelijk Onderzoek Vlaanderen'' (FWO Project No. G.0267.04).

REFERENCES

[1] Baba M. Cellular factors as alternative targets for inhibition of HIV-1. Antiviral Res 1997;33:141–52.
[2] Baichwal VR, Baeuerle PA. Activate NF-kappa B or die? Curr Biol 1997;7:R94–6.
[3] Balzarini J, Stevens M, Andrei G, Snoeck R, Strunk R, Pierce JB, et al. Pyridine oxide derivatives: structure-activity relationship for inhibition of human immunodeficiency virus and cytomegalovirus replication in cell culture. Helv Chim Acta 2002;85:2961–74.
[4] Balzarini J, Stevens M, De Clercq E, Schols D, Pannecouque C. Pyridine *N*-oxide derivatives: unusual anti-HIV compounds with multiple mechanisms of antiviral action. J Antimicrob Chemother 2005;55:135–8.
[5] Beg AA, Ruben SM, Scheinman RI, Haskill S, Rosen CA, Baldwin Jr AS. I kappa B interacts with the nuclear localization sequences of the subunits of NF-kappa B: a mechanism for cytoplasmic retention. Genes Dev 1992;6:1899–913.
[6] Bowie A, O'Neill LAJ. Oxidative stress and nuclear factor-kappaB activation: a reassessment of the evidence in the light of recent discoveries. Biochem Pharmacol 2000;59:13–23.
[7] Butera ST, Perez VL, Wu BY, Nabel GJ, Folks TM. Oscillation of the human immunodeficiency virus surface receptor is regulated by the state of viral activation in a CD4+ cell model of chronic infection. J Virol 1991;65:4645–53.
[8] Caputo A, Sodroski JG, Haseltine WA. Constitutive expression of HIV-1 tat protein in human Jurkat T cells using a BK virus vector. J Acquir Immune Defic Syndr 1990;3:372–9.
[9] Daelemans D, De Clercq E, Vandamme AM. A quantitative GFP-based bioassay for the detection of HIV-1 Tat transactivation inhibitors. J Virol Methods 2001;96:183–8.
[10] Daelemans D, Vandamme AM, De Clercq E. Human immunodeficiency virus gene regulation as a target for antiviral chemotherapy. Antiviral Chem Chemother 1999;10:1–14.
[11] Dudley E, Hornung F, Zheng L, Scherer D, Ballard D, Lenardo M. NF-κB regulates Fas/APO-1/CD95- and TCR-mediated apoptosis of T lymphocytes. Eur J Immunol 1999;29:878–86.
[12] Flohé L, Brigelius-Flohé R, Saliou C, Traber MG, Packer L. Redox regulation of NF-kappa B activation. Free Radic Biol Med 1997;22:1115–26.
[13] Floreani M, Petrone M, Debetto P, Palatini P. A comparison between different methods for the determination of reduced and oxidized glutathione in mammalian tissues. Free Rad Res 1997;26:449–55.

[14] Folks TM, Justement J, Kinter A, Dinarello CA, Fauci AS. Cytokine-induced expression of HIV-1 in a chronically infected promonocyte cell line. Science 1987;238: 800–2.
[15] Ginn-Pease ME, Whisler RL. Redox signals and NF-κB activation in T cells. Free Radic Biol Med 1998;25:346–61.
[16] Hayashi T, Ueno Y, Okamoto T. Oxidoreductive regulation of nuclear factor κ B. J Biol Chem 1993;268:11380–8.
[17] Hayden MS, Ghosh S. Signaling to NF-κB. Genes Dev 2004;18:2195–224.
[18] Hirota K, Murata M, Sachi Y, Nakamura H, Takeuchi J, Mori K, et al. Distinct roles of thioredoxin in the cytoplasm and in the nucleus. J Biol Chem 1999;274:27891–7.
[19] Kondo T, Higashiyama Y, Goto S, Iida T, Cho S, Iwanaga M, et al. Regulation of gamma-glutamylcysteine synthetase expression in response to oxidative stress. Free Radic Res 1999;31:325–34.
[20] Kreuz S, Siegmund D, Scheurich P, Wajant H. NF-kappaB inducers upregulate cFLIP, a cycloheximide-sensitive inhibitor of death receptor signalling. Mol Cell Biol 2001;21:3964–73.
[21] Lamberti A, Romano MF, Agosti V, Garbi C, Sun SC, Bond HM, et al. Regulation of cell survival in CD95-induced T cell apoptosis: role of NF-kappa B/Rel transcription factors. Apoptosis 1999;4:179–86.
[22] Lee JI, Burckart GJ. Nuclear factor kappa B: important transcription factor and therapeutic target. J Clin Pharmacol 1998;38:981–93.
[23] Legrand-Poels S, Vaira D, Pincemail J, van de Vorst A, Piette J. Activation of human immunodeficiency virus type 1 by oxidative stress. AIDS Res Hum Retroviruses 1990;6:1389–97.
[24] Matthews JR, Wakasugi N, Virelizier JL, Yodoi J, Hay RT. Thioredoxin regulates the DNA binding activity of NF-κB by reduction of a disulphide bond involving cysteine 62. Nucleic Acids Res 1992;20:3821–30.
[25] Matthews JR, Kaszubska W, Turcatti G, Wells TNC, Hay RT. Role of cysteine$_{62}$ in DNA recognition by the P50 subunit of NF-κB. Nucleic Acids Res 1993;21:1727–34.
[26] Monks NR, Biswas DK, Pardee AB. Blocking anti-apoptosis as a strategy for cancer chemotherapy: NF-κB as a target. J Cell Biochem 2004;92:646–50.
[27] Mora AL, Corn RA, Stanic AK, Goenka S, Aronica M, Stanley S, et al. Antiapoptotic function of NF-κB in T lymphocytes is influenced by their differentiation status: roles of Fas, c-FLIP, and Bcl-x$_L$. Cell Death Differ 2003;10:1032–44.
[28] Pande V, Ramos MJ. Nuclear factor kappa B: a potential target for anti-HIV chemotherapy. Curr Med Chem 2003;10:1603–15.
[29] Pande V, Ramos MJ. NF-kappaB in human disease: current inhibitors and prospects for de novo structure based design of inhibitors. Curr Med Chem 2005;12: 357–74.
[30] Pauwels R, Balzarini J, Baba M, Snoeck R, Schols D, Herdewijn P, et al. Rapid and automated tetrazolium-based colorimetric assay for the detection of anti-HIV compounds. J Virol Methods 1988;20:309–21.
[31] Ravi R, Bedi A, Fuchs EJ, Bedi A. CD95 (Fas)-induced caspase-mediated proteolysis of NF-kappaB. Cancer Res 1998;58:882–6.
[32] Sato N, Iwata S, Nakamura K, Hori T, Mori K, Yodoi J. Thiol-mediated redox regulation of apoptosis. J Immunol 1995;154:3194–203.
[33] Staal FJT, Roederer M, Herzenberg LA, Herzenberg LA. Intracellular thiols regulate activation of nuclear factor κB and transcription of human immunodeficiency virus. Proc Natl Acad Sci USA 1990;87:9943–7.
[34] Stevens M, Pannecouque C, De Clercq E, Balzarini J. Inhibition of human immunodeficiency virus by a new class of pyridine oxide derivatives. Antimicrob Agents Chemother 2003;47:2951–7.
[35] Stevens M, Pannecouque C, De Clercq E, Balzarini J. Novel human immunodeficiency virus (HIV) inhibitors that have a dual mode of anti-HIV action. Antimicrob Agents Chemother 2003;47:3109–16.
[36] Stevens M, Balzarini J, Tabarrini O, Andrei G, Snoeck R, Cecchetti V, et al. Cell- dependent interference of a series of new 6-aminoquinolone derivatives with viral (HIV/CMV) transactivation. J Antimicrob Chemother 2005;56:847–55.
[37] Sun SC, Ganchi PA, Ballard DW, Greene WC. NF-κB controls expression of inhibitor IκBα: evidence for an inducible autoregulatory pathway. Science 1993;259: 1912–5.
[38] Toledano MB, Leonard WJ. Modulation of transcription factor NF-κB binding activity by oxidation-reduction in vitro. Proc Natl Acad Sci USA 1991;88:4328–32.
[39] Whiteside ST, Israel A. I kappa B proteins: structure, function and regulation. Semin Cancer Biol 1997;8: 75–82.
[40] Wu MX, Ao Z, Prasad KV, Wu R, Schlossman SF. IEX-1L, an apoptosis inhibitor involved in NF-kappaB-mediated cell survival. Science 1998;281:998–1001.